Propofol protects H9C2 cells against hypoxia/reoxygenation injury through miR-449a and NR4A2

QIU QIAN and YINGXIANG XIE

Department of Anesthesiology, Children's Hospital of Soochow University, Suzhou, Jiangsu 215000, P.R. China

Abstract. Propofol has been revealed to protect cardio-myocytes against myocardial ischemia injury, although the underlying mechanism remains incompletely understood. H9C2 cells were used to generate a hypoxia/reoxygenation (H/R) *in vitro* model for the present study. Reverse transcription-quantitative PCR and western blotting were performed to measure the expression levels of microRNA (miR)-449a and nuclear receptor subfamily 4 group A member 2 (NR4A2). The CCK-8, BrdU, EdU, and caspase-3 activity assays and western blot analysis were employed to detect cell viability, proliferation, and apoptosis. The target relationship between miR-449a and NR4A2 was verified through dual-luciferase reporter assays. The results confirmed that exposure of the cells to H/R resulted in severe cell injury. However, the presence of propofol improved cell activity by promoting cell viability and proliferation and inhibiting cell apoptosis. The beneficial effect of propofol on H/R-mediated injury could be abrogated by the inhibition of NR4A2 mediated by miR-449a. Thus, the present study demonstrated that propofol counter-acted cardiomyocyte H/R injury by inhibiting miR-449a to upregulate NR4A2.

Introduction

Myocardial ischemia, a consequence of the blockage of arteries, is believed to be a common and major cause of high mortality in patients with heart disease worldwide (1). Reperfusion of the ischemic area is an effective way to save patients, but it can potentially lead to additional heart damage termed myocardial ischemia/reperfusion (I/R) injury (2). Myocardial I/R injury usually contributes to the exacerbation of heart disease by causing cardiac arrhythmias, myocardial infarction, and even sudden death (3). To date, the application of ischemic post-conditioning is believed to be a promising cardioprotective intervention that can reduce myocardial I/R injury (4,5). One commonly used *in vitro* model for the investigation of the mechanisms of I/R injury is the hypoxia/reoxygenation (H/R) injury model (6-8).

Propofol is a widely adopted intravenous anesthetic. It functions as a novel ischemic postconditioning agent by exhibiting a protective capability against myocardial I/R injury (9-12). It is reported that propofol possesses antioxidant capacity (13) and free radical scavenging activity (14) and thus ameliorates myocardial I/R injury (15). Therefore, the characterization of the molecular mechanism of propofol in exerting cardio-protection is of great significance and could provide novel applications for the treatment of myocardial I/R injury. In the present study, H9C2 cells (embryonic rat heart-derived) were cultured and exposed to H/R injury to mimic the I/R challenge and gain insights into the mechanism of propofol.

The relationship between microRNAs (miRNAs/miRs) and myocardial I/R injury is reported in emerging available data. Previous studies revealed that the concentrations of miR-145 (16), miR-327 (17), and miR-29 (18) were enriched in myocardial I/R injury, and suppression of these miRNAs improved the effect on the cardiomyocytes with I/R injury. Apart from these miRNAs, miR-449a has also been well established as a factor that aggravates hypoxia-induced damage of cardiomyocytes (19). In line with this, the detrimental effect of miR-449a on H9C2 cells subjected to H/R injury was also demonstrated in another study (20). Based on these previous reports, the present study attempted to gain a deeper insight into the role of miR-449a in myocardial I/R injury through its relationship with propofol; to the best of our knowledge, its involvement remains unclear.

Nuclear receptor subfamily 4 group A member 2 (NR4A2) is often studied in Parkinson's disease due to its roles in neuroprotection and its symptomatic improvement (21). The NR4A family consists of three members: NR4A1, NR4A2, and NR4A3. They are expressed in cardiomyocytes (22) and quickly react in response to ischemic stroke (23). A previous study reported that NR4A2 was enhanced in cardio-myocytes subjected to ischemia and exerted a suppressive effect on ischemia-induced apoptosis, which was regulated by miR-212-3p (24). The present study focused on the role of NR4A2 in H9C2 cells exposed to H/R challenge in the presence of propofol and following miR-449a expression

Correspondence to: Dr Yingxiang Xie, Department of Anesthesiology, Children's Hospital of Soochow University, Suzhou Industrial Park, 92 Zhongnan Street, Suzhou, Jiangsu 215000, P.R. China
E-mail: yingxiang_xie@163.com

manipulation. The current results may provide novel insights into the cardioprotective mechanism of propofol against I/R injury.

Materials and methods

Bioinformatics analysis. The GSE4386 dataset (25) (from the GEO DataSets; https://www.ncbi.nlm.nih.gov/gds) is a previously published mRNA microarray analysis involving atrial samples with or without propofol. The upregulated differentially expressed genes (DEGs) in atrial samples with propofol were determined by limma 3.26.8 (Bioconductor) using P<0.05 and log [fold change (FC)]≥2. The STRING (https://string-db.org/) database was then used to construct the interaction network for the top 20 upregulated DEGs to identify the key genes. Finally, the Tarbase (http://carolina.imis.athena-innovation.gr/diana_tools/web/index.php?r=tarbasev8/index) and miRDB (http://mirdb.org/) databases were used to predict the potential upstream miRNAs of the key gene.

Cell culture and H/R challenge. The H9C2 (embryonic rat heart-derived cell) cell line was purchased from the American Type Culture Collection and cultured in DMEM medium (Sigma-Aldrich; Merck KGaA) with 10% fetal bovine serum (Gibco; Thermo Fisher Scientific, Inc.) and 1% penicillin/streptomycin (Invitrogen; Thermo Fisher Scientific, Inc.) in an incubator with 5% CO_2 at 37°C. To simulate I/R injury, H/R injury was induced by placing H9C2 cells in hypoxic conditions (1% O_2, 95% N_2, and 5% CO_2) for 12 h. Then, reoxygenation was achieved by transferring the cells to normal culture conditions for 6 h. Cells in the control group were cultured normally. Propofol with concentrations of 0, 25, 50, and 100 μmol/l was added into the fresh medium before H/R challenge, and cell viability was detected by the CCK-8 assay. The dose of 50 μmol/l propofol was selected for subsequent experimental treatments.

Cell transfection. miR-449a inhibitor (cat. no. miR20001541-1-5), miR-449a mimic (cat. no. miR10001541-1-5), corresponding negative controls (mimic NC, cat. no. miR1N0000003-1-5 and inhibitor-NC, cat. no. miR2N0000003-1-5), NR4A2-targeting small interfering (si-) RNA (cat. no. siB14428110628-1-5), and non-targeting control siRNA (si-NC; cat. no. siN0000001-1-5) (all from Guangzhou RiboBio Co., Ltd.) were transfected into the H9C2 cells using the Lipofectamine™ 2000 reagent (Thermo Fisher Scientific, Inc.) at 37°C according to the manufacturer's protocol. Transfections were conducted when cells were at ~70% confluency. The transfection concentrations were 3 pmol for a 96-well plate, 30 pmol for a 12-well plate and 75 pmol for a 6-well plate. Subsequent experiments were performed at 48 h following transfection.

Reverse transcription-quantitative PCR (RT-qPCR). Total RNA was extracted using the TRIzol reagent (Invitrogen; Thermo Fisher Scientific, Inc.). To analyze miR-449a expression levels, reverse transcription was conducted using the All-in-One miRNA First-Strand cDNA Synthesis kit (GeneCopoeia, Inc.) and qPCR was performed with the All-in-One miRNA qRT-PCR Detection kit 2.0 (GeneCopoeia, Inc.). The thermocycling conditions were: 95°C initial denaturation for 10 min,

followed by 40 cycles of 95°C denaturation for 10 sec, 60°C annealing for 20 sec, and 72°C extension for 10 sec. U6 served as the internal control for miR-449a. To analyze NR4A2 mRNA expression levels, FastStart Universal SYBR Green Master (ROX) kit (Roche Diagnostics) was used. A total of 1 μl of the enzyme mix was used for 25 μl of each RT-PCR reaction. The reverse transcription step was performed at 16°C for 30 min without the RT-PCR enzyme mix, then at 42°C for 40 min with the enzyme mix, followed by 30 cycles of amplification at 95°C for 20 sec and 60°C for 1 min. GAPDH served as the internal control for mRNA detection. qPCR was performed in an ABI 7300 thermocycler (Applied Biosystems; Thermo Fisher Scientific, Inc.) and the $2^{-\Delta\Delta Cq}$ method (26) was used for quantification of the results. The primer sequences are listed in Table I.

Cell counting kit-8 (CCK-8) assay. Cell viability was assessed by the CCK-8 assay (MedChemExpres). H9C2 cells were plated in 96-well plates at $2x10^3$ cells/well. The detection time points were set at 1, 6, 12, 24, and 48 h post-transfection. For detection, cells were treated with 100 μl of the CCK-8 solution for 4 h, and optical density was measured using a microplate reader (BioTek Instruments, Inc.) at the wavelength of 450 nm.

BrdU assay. The proliferation of H9C2 cells was detected by the Cell Proliferation Assay kit (Cell Signaling Technology, Inc.). Briefly, 10 μM of BrdU solution was added into each well (containing $2x10^3$ H9C2 cells/well) in a 96-well plate and incubated for 2 h. Next, the absorbance at 450 nm was determined using a microplate reader (BioTek Instruments, Inc.).

EdU assay. H9C2 cells were seeded in 96-well plates at a density of $5x10^3$ cells/well for 48 h and cell proliferation was evaluated using the Cell-Light EdU Apollo567 kit (Guangzhou RiboBio Co., Ltd.). Briefly, 50 μmol/l of EdU was added into the cell culture medium and incubated for 2 h. The cells were then treated with 4% paraformaldehyde for 30 min and 0.5% Triton X-100 for 20 min. After washing with PBS, the cells were stained at room temperature for 30 min with the anti-EdU working solution and incubated with 100 μl of the Hoechst 33342 stain (5 μg/ml). Finally, a fluorescence microscope (Olympus Corporation) was used to capture images of the cells, and the percentage of EdU-positive cells was calculated from 5 optical fields/well.

Caspase-3 activity assay. Cell apoptosis was evaluated using the Caspase-3 Activity Assay kit (Cell Signaling Technology, Inc.). H9C2 cells ($2x10^3$ cells/well) were cultured in 96-well plates. Briefly, the collected cells were lysed with the lysis buffer. Then, 0.2 mM of the caspase-3 substrate Ac-DEVD-pNA was added into the cell supernatant obtained from high-speed centrifugation and incubated for 2 h at 37°C. Finally, caspase-3 activity was determined at 405 nm using a microplate reader (BioTek Instruments, Inc.).

Dual-luciferase reporter assay. The NR4A2 wild-type (wt) sequence containing the predicted miR-449a binding sites, and a NR4A2 mutant (mut) sequence containing the altered miR-449a binding sites, were amplified by PCR and

Table I. Sequences of primers used in reverse transcription-quantitative PCR.

Gene	Primer	Sequence (5'-3')
miR-449a	Forward	GCAGTGTATTGTTAGCTG
	Reverse	GAACATGTCTGCGTATCTC
U6	Forward	CTCGCTTCGGCAGCACA
	Reverse	AACGCTTCACGAATTTGCGT
NR4A2	Forward	AAACTGCCCAGTGGACAAGCGT
	Reverse	GCTCTTCGGTTTCGAGGGCAAA
GAPDH	Forward	CACCATTGGCAATGAGCGGTTC
	Reverse	AGGTCTTTGCGGATGTCCACGT

miR, microRNA; NR4A2, nuclear receptor subfamily 4 group A member 2.

subcloned into the pGL3 luciferase reporter vectors (Promega Corporation). The mutant miR-449a binding sites were produced by replacing GUGACGG with CCCUUAA. Next, the constructed NR4A2 wt or NR4A2 mut reporters were co-transfected into the H9C2 cells together with the miR-449a mimic or the negative control using the Lipofectamine 2000 reagent (Thermo Fisher Scientific, Inc.). After 48 h of the co-transfection, the relative luciferase activity was determined using the dual-luciferase reporter assay (Promega Corporation). Firefly luciferase activity was normalized to *Renilla* luciferase activity.

Western blotting. Cells were lyzed by using an ice-cold RIPA buffer (Thermo Fisher Scientific, Inc.) containing the protease inhibitor phenylmethylsulfonyl fluoride. The concentrations of total proteins were analyzed using a bicinchoninic acid protein assay kit (Thermo Fisher Scientific, Inc.). An equal amount of protein (20 μg/lane) was analyzed by 12% SDS-PAGE for 1-h separation at 100 V. After separation, the proteins were transferred onto polyvinylidene difluoride membranes and then blocked in 5% skimmed milk for 2 h at room temperature. After blocking, the membranes were incubated overnight at 4˚C with primary antibodies against NR4A2 (cat. no. bs-0178R; 1:2,000; Bioss), Bax (cat. no. bs-20377R; 1:1,000; Bioss), Bcl-2 (cat. no. bs-20351R; 1:2,000; Bioss), cleaved caspase-3 (cat. no. ab32042; 1:500; Abcam), total caspase-3 (cat. no. ab32351; 1:5,000; Abcam), and GAPDH (cat. no. ab9485; 1:2,000; Bioss). After washing, the membranes were treated with horseradish peroxidase-conjugated goat anti-rabbit IgG secondary antibody (cat. no. ab6721; 1:1,0000; Bioss) for 1 h at 37˚C. The protein bands were detected in an Odyssey CLx Infrared Imaging System (LI-COR Biosciences). The images were analyzed using ImageJ 1.8.0 (National Institutes of Health).

Statistical analysis. Data from three independent experiments were represented as the mean ± SD. All statistical tests were performed using GraphPad Prism version 8.0 (GraphPad Software, Inc.). One-way ANOVA followed by Dunnett's multiple comparisons was used to analyze the differences among multiple experimental groups. Unpaired student's t-test was used to analyze the differences between two experimental groups. P<0.05 was considered to indicate a statistically significant difference.

Results

Identification of the genes of interest in the present study. First, the top 20 upregulated DEGs from the GSE4386 dataset were acquired with the criteria of adjusted P-value <0.05 and log[FC]≥2 (Table II). These 20 genes were then used as input for STRING analysis to discover their interaction network (Fig. 1A). Notably, among the top 14 genes, RT-qPCR result showed that NR4A2 mRNA expression levels were found to be the lowest in H9C2 cells treated with H/R compared with control cells (Table SI). NR4A2 has been studied previously in myocardial infarction injury (24). Propofol is considered to be a cardioprotective reagent (9,10). However, the involvement of NR4A2 in cardioprotection in the presence of propofol has not been studied yet. To explore the potential roles of miRNAs in the effects of NR4A2, the potential miRNAs upstream of NR4A2 were predicted using the Tarbase and miRDB databases; seven common miRNAs were identified (Fig. 1B). Among them, miR-449a was reported to enhance the damage of cardiomyocytes (19,20). However, the involvement of miR-449a in damaging the cardiomyocytes in the presence of propofol is not clear. Therefore, the present study aimed to explore the potential interaction between miR-449a and NR4A2 on cardiomyocyte injury in the presence of propofol.

Propofol treatment exhibits a protective effect on the survival of the H9C2 cells. The CCK-8 assay was performed in the presence of different concentrations of propofol (0, 25, 50 and 100 μmol/l) to detect changes in the cell viability of H/R-induced H9C2 cells. The dose of 50 μmol/l propofol resulted in the highest cell viability and protection of H/R-induced H9C2 cells (Fig. S1). Therefore, 50 μmol/l of propofol was used for subsequent experiments. The viability of the H9C2 cells subjected to H/R treatment was dramatically reduced compared to the cells cultured normally (Fig. 2A), confirming the successful generation of the *in vitro* I/R injury model. When propofol was introduced, the cell viability of the H/R-induced cells was significantly improved (Fig. 2A). Furthermore, the proliferation rates of the H9C2 cells were also evaluated using an EdU assay. Compared with the control group, the rate of EdU-positive cells in the H/R alone group was decreased by 50%, while the rate of EdU-positive cells in the propofol-treated groups was reduced by 20% (Fig. 2B). The proliferation of the H9C2 cells detected by a BrdU assay exhibited a similar trend; the proliferation of the cells subjected to H/R alone was suppressed by 50% compared with the control group, while propofol compromised this reduction by 30% compared with the H/R group (Fig. 2C). Cell apoptosis of the H9C2 cells was measured by the caspase-3 activity assay. Caspase-3 activity of the cells in the H/R group was almost thrice as much as that of the control group; this increase was attenuated by ~50% compared with that of the H/R group when propofol was introduced (Fig. 2D). Finally, the levels of the apoptosis-associated proteins Bax, Bcl-2, and cleaved caspase-3 were detected by western blot analysis. Compared with the control group, the protein expression levels of Bax and cleaved caspase-3 were increased in the H/R group, while Bcl-2 protein expression

Table II. Top 20 differentially expressed genes from analysis of the GSE4386 data series.

| Probe ID	Adjusted P-value	P-value	Log fold change	Gene symbol	Gene full name
205207_at	2.25×10^{-15}	1.24×10^{-19}	9.036459	IL6	Interleukin 6
202768_at	3.99×10^{-14}	2.93×10^{-18}	8.554949	FOSB	FosB proto-oncogene, AP-1 transcription factor subunit
202859_x_at	2.83×10^{-12}	5.19×10^{-16}	7.785047	CXCL8	C-X-C motif chemokine ligand 8
207978_s_at	3.46×10^{-21}	6.34×10^{-26}	7.310244	NR4A3	Nuclear receptor subfamily 4 group A member 3
209189_at	5.55×10^{-07}	1.30×10^{-09}	7.065234	FOS	Fos proto-oncogene, AP-1 transcription factor subunit
206211_at	1.48×10^{-11}	4.61×10^{-15}	7.042325	SELE	Selectin E
206115_at	8.23×10^{-09}	9.80×10^{-12}	6.660009	EGR3	Early growth response 3
209774_x_at	5.44×10^{-11}	2.69×10^{-14}	6.547871	CXCL2	C-X-C motif chemokine ligand 2
236523_at	3.40×10^{-06}	9.90×10^{-09}	6.349735	LOC285556	Uncharacterized LOC285556
206932_at	3.68×10^{-13}	4.04×10^{-17}	6.310222	CH25H	Cholesterol 25-hydroxylase
207526_s_at	6.09×10^{-08}	1.07×10^{-10}	6.109762	IL1RL1	Interleukin 1 receptor like 1
227697_at	3.71×10^{-13}	4.76×10^{-17}	6.019778	SOCS3	Suppressor of cytokine signaling 3
243296_at	8.50×10^{-12}	2.02×10^{-15}	5.966462	NAMPT	Nicotinamide phosphoribosyltransferase
202628_s_at	4.18×10^{-08}	6.66×10^{-11}	5.96427	SERPINE1	Serpin family E member 1
202672_s_at	1.25×10^{-11}	3.56×10^{-15}	5.878868	ATF3	Activating transcription factor 3
212657_s_at	7.31×10^{-09}	8.17×10^{-12}	5.761876	IL1RN	Interleukin 1 receptor antagonist
201109_s_at	3.32×10^{-11}	1.28×10^{-14}	5.700034	THBS1	Thrombospondin 1
1569003_at	1.19×10^{-10}	6.31×10^{-14}	5.691674	VMP1	Vacuole membrane protein 1
216598_s_at	7.95×10^{-09}	9.31×10^{-12}	5.687414	CCL2	C-C motif chemokine ligand 2
216248_s_at	3.72×10^{-09}	3.14×10^{-12}	5.600101	NR4A2	Nuclear receptor subfamily 4 group A member 2
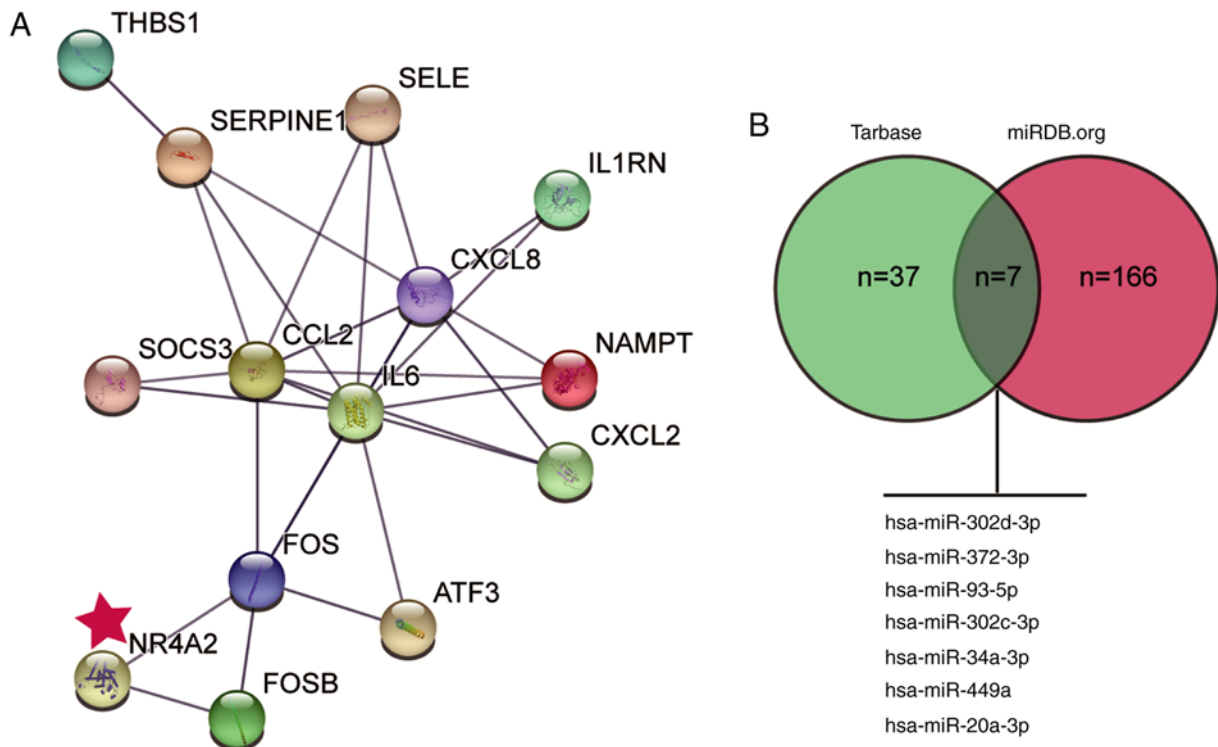
Figure 1. Identification of genes of interest. (A) STRING analysis of the top 20 upregulated genes from the GSE4386 microarray database. (B) Venn diagram showing the miRNAs predicted to be upstream of NR4A2 using the Tarbase and miRDB databases. miR, microRNA; NR4A2, nuclear receptor subfamily 4 group A member 2.
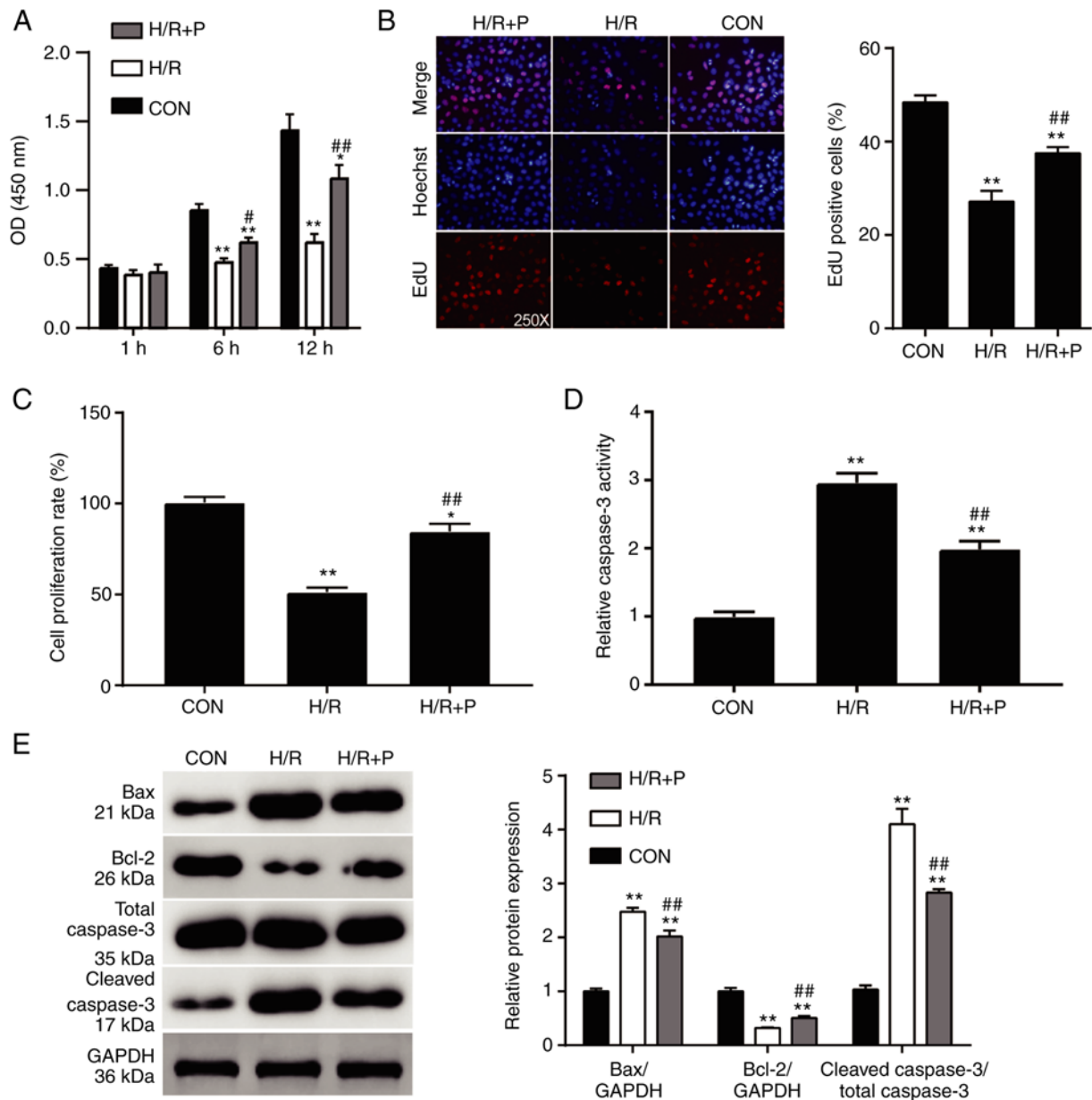
Figure 2. Propofol treatment exhibits a protective effect on the survival of H9C2 cells. H9C2 cells were subjected to H/R in the presence of absence or propofol, and phenotypic assays were performed. (A) Cell viability was measured by CCK-8 assay. (B) Cell proliferation was measured by EdU assay and by (C) BrdU assay. (D) Cell apoptosis was measured by caspase-3 activity assay. (E) Western blot analysis of Bax, Bcl-2 and cleaved caspase-3 protein expression levels. Data are presented as mean ± SD (n=3). *P<0.05, **P<0.001 compared with control. #P<0.05, ##P<0.001 vs. H/R. H/R, hypoxia/reoxygenation; P, propofol; Con, control; OD, optical density.

was decreased (Fig. 2E). Propofol treatment resulted in lower increases in the Bax and cleaved caspase-3 concentrations and a lower reduction in Bcl-2 (Fig. 2E). Together, these results demonstrated that propofol exerted a protective effect on the survival and proliferation of H9C2 cells.

Propofol attenuates H/R injury through the inhibition of miR-449a. As shown in Fig. 3A, the expression levels of miR-449a in the H/R group were ~2.7 times higher compared with the control group. The expression was relatively lower in the H/R+P group compared with that of the H/R group (1.7-fold compared with the control group; Fig. 3A). To explore the function of miR-449a, a specific inhibitor was used to down-regulate its expression. First, successful transfection efficiency

of the miR-449a inhibitor was confirmed in H9C2 cells under normoxic conditions (Fig. S2A). Next, the miR-449a inhibitor was used in the *in vitro* I/R model. Compared with H/R+P group, the expression of miR-449a in H/R+P+miR-449a inhibitor group was decreased by 50%, indicating successful downregulation of miR-449a (Fig. 3B).

Functional assays were then performed to assess the role of miR-449a. The CCK-8 assay depicted that the miR-449a inhibitor contributed to improved cell viability of the H9C2 cells treated with H/R and propofol (Fig. 3C). The EdU assay demonstrated that the miR-449a inhibitor increased the ratios of EdU-positive cells by 1.2-fold compared with those in the H/R+P group (Fig. 3D). The BrdU assay showed that, despite the severe damage caused by H/R exposure, the miR-449a
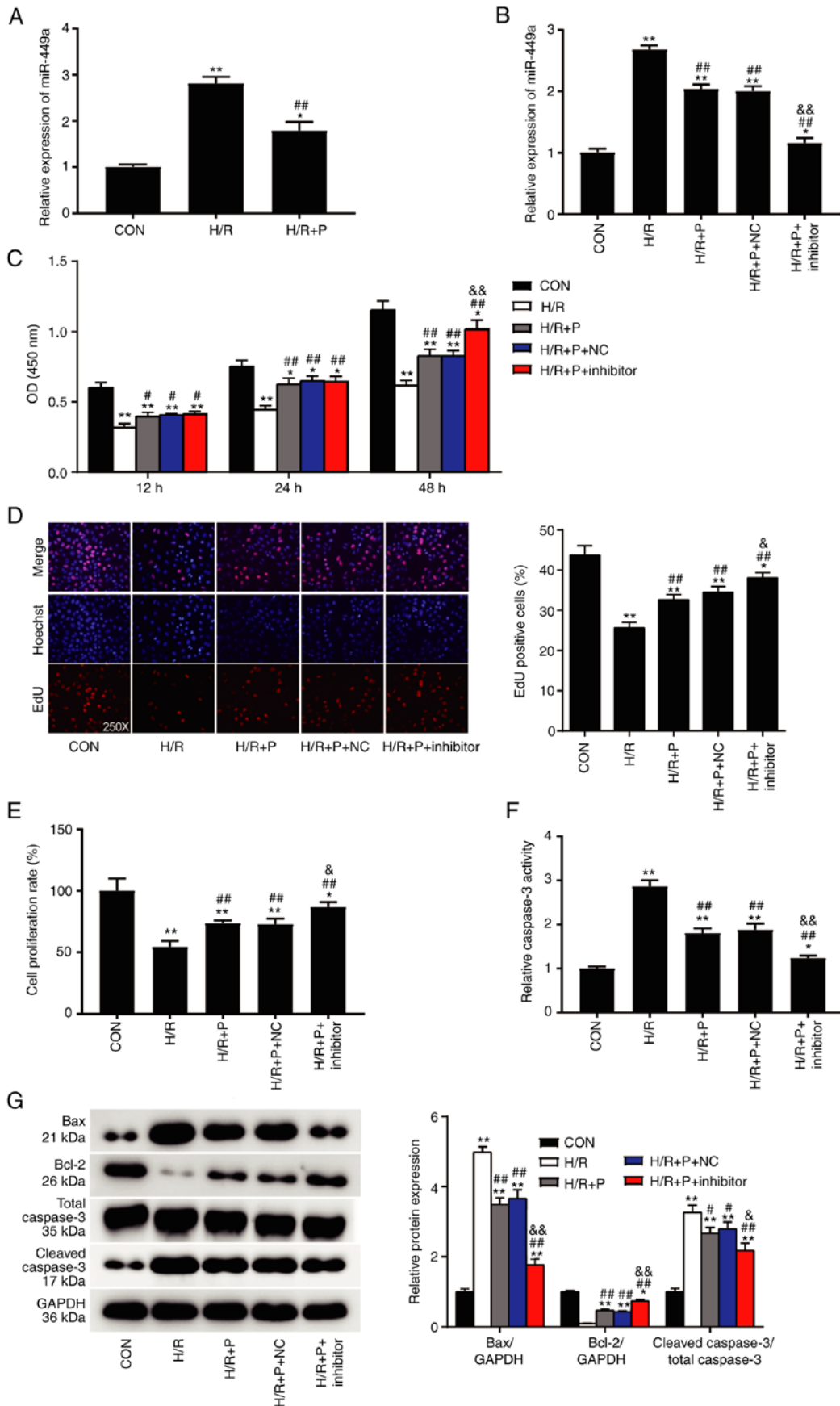
Figure 3. Propofol attenuates H/R injury through inhibition of miR-449a. (A) miR-449a expression levels in H9C2 cells were detected by RT-qPCR. (B) The transfection efficiency of miR-449a inhibitor was confirmed by RT-qPCR. (C) The effect of miR-449a inhibition on cell viability of H9C2 cells subjected to H/R injury was measured by CCK-8 assay. (D) Cell proliferation was measured by EdU assay and by (E) BrdU assay. (F) Cell apoptosis was measured by caspase-3 activity assay. (G) Western blot analysis of Bax, Bcl-2 and cleaved caspase-3 protein expression levels Data are presented as mean ± SD (n=3). *P<0.05, **P<0.001 compared with control. #P<0.05, ##P<0.001 vs. H/R. &P<0.05, &&P<0.001 vs. H/R+P+NC. H/R, hypoxia/reoxygenation; miR, microRNA; RT-qPCR, reverse transcription-quantitative PCR; P, propofol; Con, control; NC, negative control; OD, optical density.

inhibitor was able to promote cell proliferation of the H9C2 cells by 25% compared with that observed in the H/R+P group (Fig. 3E). The caspase-3 activity assay revealed that cell apoptosis was repressed in the miR-449a inhibitor group by 30% compared with that in the H/R+P group (Fig. 3F). Western blot analysis showed that the protein expression levels of Bax and cleaved caspase-3 decreased while the protein expression of Bcl-2 increased in the miR-449a inhibitor group compared with the H/R+P group (Fig. 3G). Therefore, the present results demonstrated that propofol protected H9C2 cells from H/R injury through the inhibition of miR-449a.

NR4A2 is a target gene of miR-449a in H9C2 cells. miR449a was predicted to target the NR4A2 gene (Fig. 1). To understand the mechanism underlying the action of miR-449a in H9C2 cell damage caused by H/R, the functional association between miR449a and NR4A2 was further investigated. The mRNA expression levels of NR4A2 were measured in the H/R group and the H/R+P group by RT-qPCR. The results demonstrated that NR4A2 mRNA expression was significantly higher in the H/R+P group compared with that in the H/R group (Fig. 4A). Western blot analysis further confirmed that the protein expression levels of NR4A2 in the H/R+P group was higher compared with that in the H/R group (Fig. 4B). The predicted binding sites of miR-449a on NR4A2 are depicted in Fig. 4C. As shown in Fig. 4D, luciferase activity from a wt NR4A2 reporter plasmid was repressed when co-transfected with miR-449a mimics compared with mimics NC, while no effect was observed on the luciferase activity of a mutant reporter plasmid. These results confirmed that NR4A2 was a direct target of miR-449a.

Next, NR4A2 was silenced by transfection with a specific siRNA. First, the knockdown efficiency was confirmed in H9C2 cells under normoxic conditions (Fig. S2B and C). In addition, NR4A2 siRNA transfection could significantly reduce the NR4A2 expression at the mRNA (Fig. 4E) as well as protein levels (Fig. 4F) under the H/R and propofol treatment conditions. Collectively, these results revealed that miR-449a targeted NR4A2 in the propofol protection against H/R injury in H9C2 cells.

NR4A2 exerts a protective effect on H9C2 cells mediated by miR-449a. Given that miR-449a can target NR4A2, further experiments were designed to explore if NR4A2 had a positive impact on the viability of H9C2 cells after exposure to H/R injury. The CCK-8 assay revealed that NR4A2 silencing dramatically repressed the cell viability of the H9C2 cells with H/R injury and propofol, while this repression could be restored by the miR-449a inhibitor (Fig. 5A). In the EdU assay, NR4A2 silencing reduced the ratio of EdU-positive cells in the H/R injury and propofol-treated group, while the miR-449a inhibitor reversed this reduction (Fig. 5B). The BrdU assay indicated that NR4A2 silencing hindered cell proliferation of the H9C2 cells by 20% compared with that of the H/R+P group, which was 40% lower than that of the control group (Fig. 5C). However, this repression could be restored by the miR-449a inhibitor (Fig. 5B). The Caspase-3 activity assay demonstrated that NR4A2 silencing induced apoptosis by 3-fold of the H9C2 cells in the H/R group compared with that in the control. However, this promotion could be reversed by the miR-449a inhibitor (Fig. 5D). Western blot analysis showed that the protein expression levels of Bax and cleaved caspase-3 in the H9C2 cells following NR4A2 silencing were increased compared with those in the H/R+P group, while the expression levels of Bcl-2 were decreased (Fig. 5E). Of note, the miR-449a inhibitor reversed these effects (Fig. 5E). Taken together, the current results indicated that NR4A2 exerted a protective effect on H9C2 cells, and this effect was regulated by miR-449a.

Discussion

In the present study, H/R-induced H9C2 cells were used to mimic I/R injury *in vitro*. It was observed that propofol treatment significantly alleviated H/R injury in cardiomyocytes, by improving cell viability and proliferation while repressing cell apoptosis of the H9C2 cells. Additionally, the present results suggested that the cardioprotective effect of propofol was closely related to the regulation of miR-449a and its target gene NR4A2. Specifically, miR-449a inhibition promoted cell viability and proliferation and repressed cell apoptosis of the H9C2 cells, thus enhancing the cardioprotective effect of propofol. By contrast, silencing of NR4A2, the target gene of miR-449a, hindered the alleviation effect of propofol on H/R injury.

According to previous studies, it is established that propofol protects cells against oxidative stress from hydrogen peroxide (27,28) and oxygen-glucose deprivation (29). The present results further confirmed the cell-protective role of propofol. Propofol-dependent mechanisms have been reported in several studies concerning myocardial I/R injury. A previous study reported that propofol exerted cardioprotection against myocardial I/R injury through the miR-451/HMGB1 axis in a H/R injury model of H9C2 cardiomyocytes (10). Another study reported that propofol exerted a protective effect on the H/R-challenged cardiomyocytes by activation of Akt phosphorylation (30). The present study confirmed that propofol was significantly beneficial to the survival and activity of cardiomyocytes subjected to H/R injury. The benefits of propofol could be enhanced by miR-449a inhibition and hindered by NR4A2 silencing.

miR-449a has been widely studied in various cancer models and acts as a tumor suppressor. For example, the tumor-suppressive role of miR-449a has been demonstrated in breast cancer via targeting PLAG1 like zinc finger 2 (31). In addition, miR-449a was demonstrated to be sponged by circGFRA1, thus hindering the inhibition effect of miR-449a on ovarian cancer progression (32). The role of miR-449a in cancer has been studied extensively. However, the contribution of miR-449a in protecting the heart from myocardial I/R injury or H/R injury needs further research. Two studies determined that the downregulation of miR-449a helped to protect cardiomyocytes from H/R injury (19,20). The current study also described that the inhibition of miR-449a enhanced the cardioprotective effect in the H9C2 cells against the stress from H/R injury. It was observed that miR-449a inhibition could not only promote cell viability and proliferation but also inhibit cell apoptosis in H9C2 cells.

To further elucidate the role of miR-449a in cardiomyocyte protection from H/R injury, NR4A2 was predicted and
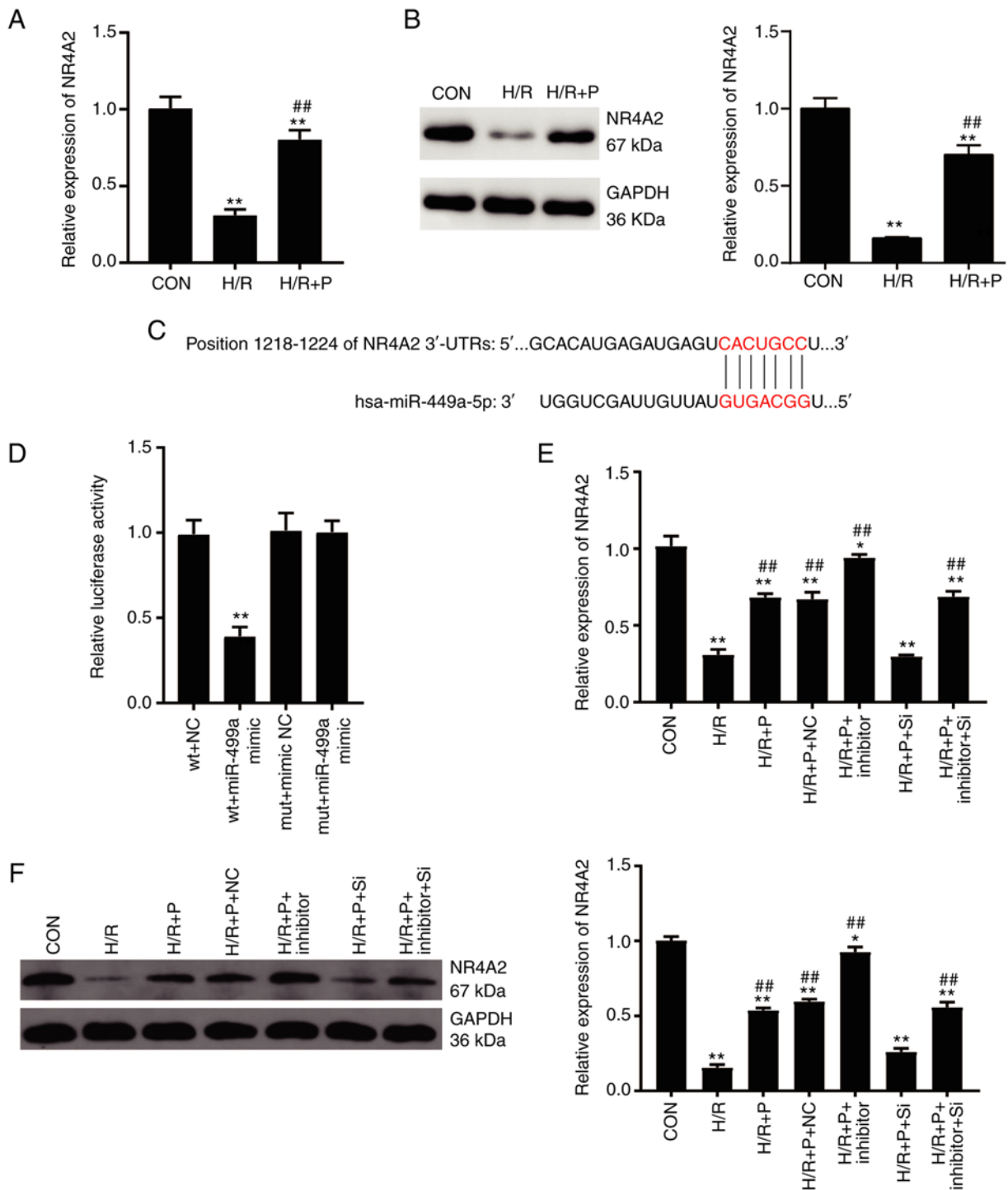
Figure 4. NR4A2 is a target gene of miR-449a. (A) NR4A2 mRNA expression levels in H9C2 cells were detected by RT-qPCR. (B) NR4A2 protein expression levels in H9C2 cells were detected by western blotting. (C) Schematic of the predicted binding sites between miR-449a and the NR4A2 3'-UTR. (D) Dual-luciferase reporter assay was performed to confirm the target relationship between miR-449a and NR4A2. (E) NR4A2 mRNA expression levels were detected by RT-qPCR following siRNA transfection. (F) NR4A2 protein expression levels were detected by western blotting following siRNA transfection. Data are presented as mean ± SD (n=3). *P<0.05, **P<0.001 compared with control. ##P<0.001 vs. H/R. NR4A2, nuclear receptor subfamily 4 group A member 2; miR, microRNA; RT-qPCR, reverse transcription-quantitative PCR; UTR, untranslated region; siRNA, small interfering RNA; Con, control; H/R, hypoxia/reoxygenation; P, propofol; wt, wild-type; mut, mutant; NC, negative control; si-NC, negative control siRNA; si, NR4A2-targeting siRNA.

confirmed as a target gene for miR-449a. A previous study determined that there was a close relationship between the haplotypes of the NR4A2 gene and cardiovascular disease (33). The role of NR4A2 in cardiomyocyte apoptosis has been illustrated previously (24), showing that NR4A2 knockdown aggravated the cardiomyocyte apoptosis in response to I/R injury. The present study clarified the function of NR4A2 in cardiomyocyte survival from the aspect of cell viability, proliferation, and apoptosis. NR4A2 was able to impede cell apoptosis of cardiomyocytes following H/R injury. This apoptosis-suppressive effect of NR4A2 was consistent with previous literature (24). In addition to the suppression of cell apoptosis, the present results
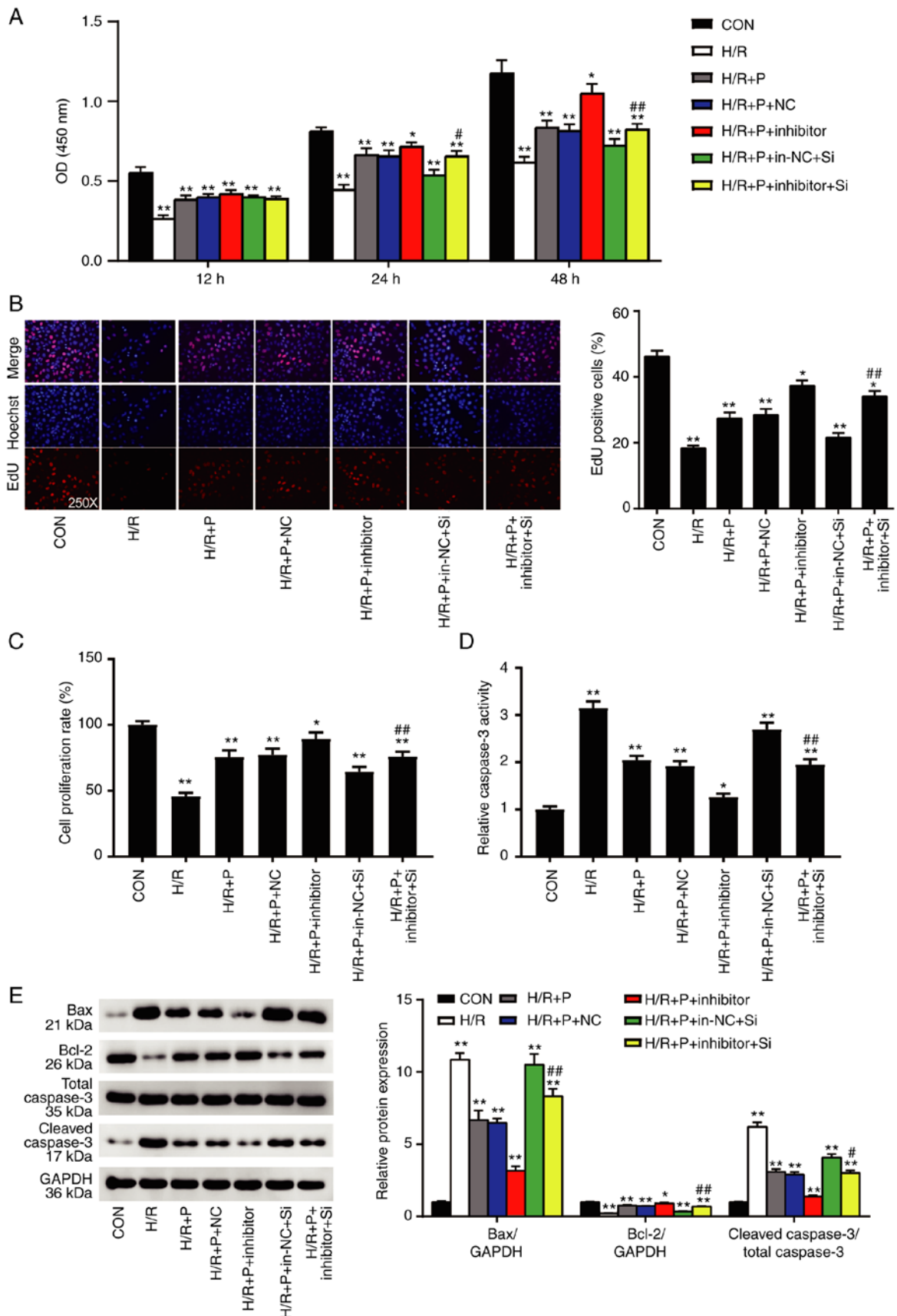
Figure 5. NR4A2 exerts a protective effect on H9C2 cells mediated by miR-449a. H9C2 cells were subjected to H/R injury in the presence or absence of propofol, and co-transfected with miR-449a inhibitor and/or NR4A2-targeting siRNA or their respective controls. (A) Cell viability was measured by CCK-8 assay. (B) Cell proliferation was measured by EdU assay and by (C) BrdU assay. (D) Apoptosis was measured by caspase-3 activity assay. (E) Western blot analysis of Bax, Bcl-2 and cleaved caspase-3 protein expression levels. Data are presented as mean ± SD (n=3). *P<0.05, **P<0.001 compared with control. #P<0.05, ##P<0.001 vs. H/R+P+in-NC+Si. NR4A2, nuclear receptor subfamily 4 group A member 2; miR, microRNA; siRNA, small interfering RNA; Con, control; H/R, hypoxia/reoxygenation; P, propofol; NC, negative control; in-NC, inhibitor negative control. si-NC, negative control siRNA; si, NR4A2-targeting siRNA.

determined a promotional effect of NR4A2 on cell viability and proliferation. Collectively, NR4A2 protected H9C2 cells from H/R injury, which was consistent with the role of propofol but opposite to that of miR-449a.

The present study explored the mechanism of propofol in H/R-mediated cell injury, but certain limitations remain. First, the present study was performed *in vitro*, and there is a lack of *in vivo* experiments to further confirm the effects of propofol and miR-449a/NR4A2 on myocardial I/R injury. In addition, the effects of propofol and miR-449a/NR4A2 on myocardial I/R injury need to be further explored in clinical samples. Further studies are underway to investigate the effects of propofol and miR-449a/NR4A2 on myocardial I/R injury *in vivo*.

In summary, the present results elucidated how propofol, miR-449a, and its target gene NR4A2 interact in protecting cardiomyocytes subjected to H/R injury. The observations can serve as a novel clue in designing therapeutic strategies for cardiovascular diseases against myocardial I/R injury.

Acknowledgements

Funding

Availability of data and materials

All data generated or analyzed during this study are included in this published article.

Authors' contributions

QQ performed the experiments and data analysis. YX conceived and designed the study. QQ wrote the paper. YX reviewed and edited the manuscript. All authors read and approved the manuscript. QQ and YX confirm the authenticity of all the raw data.

Ethics approval and consent to participate

Not applicable.

Patient consent for publication

Not applicable.

Competing interests

The authors declare that they have no competing interests.

References

1. Nadatani Y, Watanabe T, Shimada S, Otani K, Tanigawa T and Fujiwara Y: Microbiome and intestinal ischemia/reperfusion injury. J Clin Biochem Nutr 63: 26-32, 2018.
2. Binder A, Ali A, Chawla R, Aziz HA, Abbate A and Jovin IS: Myocardial protection from ischemia-reperfusion injury post coronary revascularization. Expert Rev Cardiovasc Ther 13: 1045-1057, 2015.
3. Ferdinandy P, Schulz R and Baxter GF: Interaction of cardiovascular risk factors with myocardial ischemia/reperfusion injury, preconditioning, and postconditioning. Pharmacol Rev 59: 418-458, 2007.
4. Zhao ZQ and Vinten-Johansen J: Postconditioning: Reduction of reperfusion-induced injury. Cardiovasc Res 70: 200-211, 2006.
5. Qiao SG, Sun Y, Sun B, Wang A, Qiu J, Hong L, An JZ, Wang C and Zhang HL: Sevoflurane postconditioning protects against myocardial ischemia/reperfusion injury by restoring autophagic flux via an NO-dependent mechanism. Acta Pharmacol Sin 40: 35-45, 2019.
6. Li Z, Zhang Y, Ding N, Zhao Y, Ye Z, Shen L, Yi H and Zhu Y: Inhibition of lncRNA XIST improves myocardial I/R injury by targeting miR-133a through inhibition of autophagy and regulation of SOCS2. Mol Ther Nucleic Acids 18: 764-773, 2019.
7. Yao L, Chen H, Wu Q and Xie K: Hydrogen-rich saline alleviates inflammation and apoptosis in myocardial I/R injury via PINK-mediated autophagy. Int J Mol Med 44: 1048-1062, 2019.
8. Li W, Li Y, Chu Y, Wu W, Yu Q, Zhu X and Wang Q: PLCE1 promotes myocardial ischemia-reperfusion injury in H/R H9c2 cells and I/R rats by promoting inflammation. Biosci Rep 39: BSR20181613, 2019.
9. Lotz C, Stumpner J and Smul TM: Sevoflurane as opposed to propofol anesthesia preserves mitochondrial function and alleviates myocardial ischemia/reperfusion injury. Biomed Pharmacother 129: 110417, 2020.
10. Li YM, Sun JG, Hu LH, Ma XC, Zhou G and Huang XZ: Propofol-mediated cardioprotection dependent of microRNA-451/HMGB1 against myocardial ischemia-reperfusion injury. J Cell Physiol 234: 23289-23301, 2019.
11. Li H, Zhang X, Tan J, Sun L, Xu LH, Jiang YG, Lou JS, Shi XY and Mi WD: Propofol postconditioning protects H9c2 cells from hypoxia/reoxygenation injury by inducing autophagy via the SAPK/JNK pathway. Mol Med Rep 17: 4573-4580, 2018.
12. Zhao D, Li Q, Huang Q, Li X, Yin M, Wang Z and Hong J: Cardioprotective effect of propofol against oxygen glucose deprivation and reperfusion injury in H9c2 cells. Oxid Med Cell Longev 2015: 184938, 2015.
13. Vasileiou I, Xanthos T, Koudouna E, Perrea D, Klonaris C, Katsargyris A and Papadimitriou L: Propofol: A review of its non-anaesthetic effects. Eur J Pharmacol 605: 1-8, 2009.
14. Green TR, Bennett SR and Nelson VM: Specificity and properties of propofol as an antioxidant free radical scavenger. Toxicol Appl Pharmacol 129: 163-169, 1994.
15. Hanouz JL, Yvon A, Flais F, Rouet R, Ducouret P, Bricard H and Gérard JL: Propofol decreases reperfusion-induced arrhythmias in a model of 'border zone' between normal and ischemic-reperfused guinea pig myocardium. Anesth Analg 97: 1230-1238, 2003.
16. Hu S, Cao S, Tong Z and Liu J: FGF21 protects myocardial ischemia-reperfusion injury through reduction of miR-145-mediated autophagy. Am J Transl Res 10: 3677-3688, 2018.
17. Yang Y, Yang J, Liu XW, Ding JW, Li S, Guo X, Yang CJ, Fan ZX, Wang HB, Li Q, et al: Down-regulation of miR-327 alleviates ischemia/reperfusion-induced myocardial damage by targeting RP105. Cell Physiol Biochem 49: 1049-1063, 2018.
18. Ye Y, Hu Z, Lin Y, Zhang C and Perez-Polo JR: Downregulation of microRNA-29 by antisense inhibitors and a PPAR-gamma agonist protects against myocardial ischaemia-reperfusion injury. Cardiovasc Res 87: 535-544, 2010.
19. Cheng J, Wu Q, Lv R, Huang L, Xu B, Wang X, Chen A and He F: MicroRNA-449a inhibition protects H9C2 cells against hypoxia/reoxygenation-induced injury by targeting the Notch-1 signaling pathway. Cell Physiol Biochem 46: 2587-2600, 2018.
20. Zhang X, Dong H, Liu Y, Han J, Tang S and Si J: Tetramethylpyrazine partially relieves hypoxia-caused damage of cardiomyocytes H9c2 by downregulation of miR-449a. J Cell Physiol, Feb 15, 2019 (Epub ahead of print).
21. Spathis AD, Asvos X, Ziavra D, Karampelas T, Topouzis S, Cournia Z, Qing X, Alexakos P, Smits LM, Dalla C, et al: Nurr1:RXRα heterodimer activation as monotherapy for Parkinson's disease. Proc Natl Acad Sci USA 114: 3999-4004, 2017.
22. Medzikovic L, Schumacher CA, Verkerk AO, van Deel ED, Wolswinkel R, van der Made I, Bleeker N, Cakici D, van den Hoogenhof MM, Meggouh F, et al: Orphan nuclear receptor Nur77 affects cardiomyocyte calcium homeostasis and adverse cardiac remodelling. Sci Rep 5: 15404, 2015.
23. Xiao G, Sun T, Songming C and Cao Y: NR4A1 enhances neural survival following oxygen and glucose deprivation: An in vitro study. J Neurol Sci 330: 78-84, 2013.

24. Liu H, Liu P, Shi X, Yin D and Zhao J: NR4A2 protects cardiomyocytes against myocardial infarction injury by promoting autophagy. Cell Death Discov 4: 27, 2018.
25. Lucchinetti E, Hofer C, Bestmann L, Hersberger M, Feng J, Zhu M, Furrer L, Schaub MC, Tavakoli R, Genoni M, et al: Gene regulatory control of myocardial energy metabolism predicts postoperative cardiac function in patients undergoing off-pump coronary artery bypass graft surgery: Inhalational versus intravenous anesthetics. Anesthesiology 106: 444-457, 2007.
26. Livak KJ and Schmittgen TD: Analysis of relative gene expression data using real-time quantitative PCR and the 2(-Delta Delta C(T)) method. Methods 25: 402-408, 2001.
27. Ming N, Na HST, He JL, Meng QT and Xia ZY: Propofol alleviates oxidative stress via upregulating lncRNA-TUG1/Brg1 pathway in hypoxia/reoxygenation hepatic cells. J Biochem 166: 415-421, 2019.
28. Kim EJ, Choi IS, Yoon JY, Park BS, Yoon JU and Kim CH: Effects of propofol-induced autophagy against oxidative stress in human osteoblasts. J Dent Anesth Pain Med 16: 39-47, 2016.
29. Wang Z, Yang P and Qi Y: Role of microRNA-134 in the neuroprotective effects of propofol against oxygen-glucose deprivation and related mechanisms. Int J Clin Exp Med 8: 20617-20623, 2015.
30. Ma K, Qiu J, Zhou M, Yang Y and Ye X: Cox-2 Negatively affects the protective role of propofol against hypoxia/reoxygenation induced cardiomyocytes apoptosis through suppressing Akt signaling. Biomed Res Int 2019: 7587451, 2019.
31. Xu B, Zhang X, Wang S and Shi B: MiR-449a suppresses cell migration and invasion by targeting PLAGL2 in breast cancer. Pathol Res Pract 214: 790-795, 2018.
32. Liu J, Yu F, Wang S, Zhao X, Jiang F, Xie J and Deng M: circGFRA1 promotes ovarian cancer progression by sponging miR-449a. J Cancer 10: 3908-3913, 2019.
33. Kardys I, van Tiel CM, de Vries CJ, Pannekoek H, Uitterlinden AG, Hofman A, Witteman JC and de Maat MP: Haplotypes of the NR4A2/NURR1 gene and cardiovascular disease: The Rotterdam Study. Hum Mutat 30: 417-423, 2009.